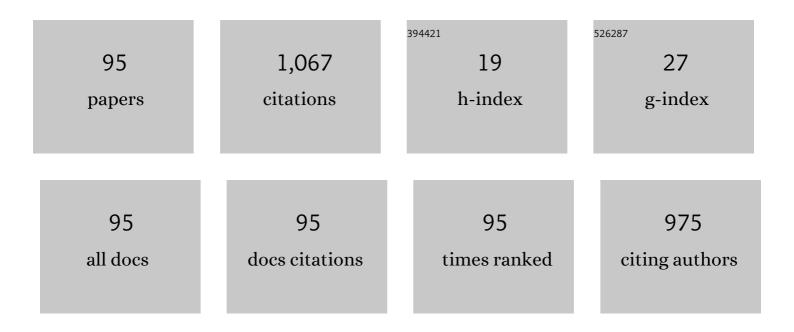
List of Publications by Year in descending order

Source: https://exaly.com/author-pdf/4027237/publications.pdf Version: 2024-02-01



Lill_AN Li

#	Article	IF	CITATIONS
1	Investigation on crystalline structure, boron distribution, and residual stresses in freestanding boron-doped CVD diamond films. Journal of Crystal Growth, 2010, 312, 1986-1991.	1.5	72
2	Fabrication, structure, and photocatalytic activities of boron-doped ZnO nanorods hydrothermally grown on CVD diamond film. Chemical Physics Letters, 2012, 539-540, 74-78.	2.6	53
3	GaN Schottky Barrier Diode With TiN Electrode for Microwave Rectification. IEEE Journal of the Electron Devices Society, 2014, 2, 168-173.	2.1	44
4	Self-powered GaN ultraviolet photodetectors with p-NiO electrode grown by thermal oxidation. Materials Science in Semiconductor Processing, 2018, 76, 61-64.	4.0	40
5	Synthesis and characterization of p-type NiO films suitable for normally-off AlGaN/GaN HFETs application. Materials Science in Semiconductor Processing, 2017, 67, 141-146.	4.0	30
6	Synthesis and properties of boron doped ZnO nanorods on silicon substrate by low-temperature hydrothermal reaction. Applied Surface Science, 2011, 257, 5984-5988.	6.1	29
7	NiO/GaN heterojunction diode deposited through magnetron reactive sputtering. Journal of Vacuum Science and Technology A: Vacuum, Surfaces and Films, 2016, 34, .	2.1	28
8	Correlation Between Anode Area and Sensitivity for the TiN/GaN Schottky Barrier Diode Temperature Sensor. IEEE Transactions on Electron Devices, 2020, 67, 1171-1175.	3.0	28
9	Process dependency on threshold voltage of GaN MOSFET on AlGaN/GaN heterostructure. Solid-State Electronics, 2014, 99, 59-64.	1.4	27
10	p-NiO/n-GaN Heterostructure Diode for Temperature Sensor Application. IEEE Sensors Journal, 2020, 20, 62-66.	4.7	27
11	Enhanced pH sensitivity of AlGaN/GaN ion-sensitive field effect transistor with Al2O3 synthesized by atomic layer deposition. Applied Surface Science, 2018, 427, 1199-1202.	6.1	26
12	Application of p-type NiO deposited by magnetron reactive sputtering on GaN vertical diodes. Materials Science in Semiconductor Processing, 2021, 125, 105628.	4.0	26
13	High Threshold Voltage Uniformity and Low Hysteresis Recessed-Gate Al ₂ O ₃ /AIN/GaN MISFET by Selective Area Growth. IEEE Transactions on Electron Devices, 2017, 64, 1554-1560.	3.0	25
14	High-Mobility Normally OFF Al ₂ O ₃ /AlGaN/GaN MISFET With Damage-Free Recessed-Gate Structure. IEEE Electron Device Letters, 2018, 39, 1720-1723.	3.9	23
15	Temperature sensor using thermally stable TiN anode GaN Schottky barrier diode for high power device application. Superlattices and Microstructures, 2018, 123, 274-279.	3.1	23
16	Fast and slow interface traps in transparent NiO gated AlGaN/GaN heterostructure field-effect transistors. Applied Surface Science, 2019, 475, 1043-1047.	6.1	22
17	Electrical properties of TiN on gallium nitride grown using different deposition conditions and annealing. Journal of Vacuum Science and Technology A: Vacuum, Surfaces and Films, 2014, 32, 02B116.	2.1	21
18	Enhanced Sensitivity of GaN-Based Temperature Sensor by Using the Series Schottky Barrier Diode Structure. IEEE Electron Device Letters, 2020, 41, 601-604.	3.9	21

#	Article	IF	CITATIONS
19	Dependence of reaction pressure on deposition and properties of boron-doped freestanding diamond films. Applied Surface Science, 2010, 256, 1764-1768.	6.1	20
20	Temperature-dependent electrical transport characteristics of a NiO/GaN heterojunction diode. Surfaces and Interfaces, 2016, 5, 15-18.	3.0	19
21	Threshold voltage tuning in AlGaN/GaN HFETs with p-type Cu2O gate synthesized by magnetron reactive sputtering. Applied Surface Science, 2018, 437, 98-102.	6.1	19
22	Normally-Off AlGaN/GaN Heterojunction Metal-Insulator-Semiconductor Field-Effect Transistors With Gate-First Process. IEEE Electron Device Letters, 2019, 40, 185-188.	3.9	19
23	Effect of thermal oxidation treatment on pH sensitivity of AlGaN/GaN heterostructure ion-sensitive field-effect transistors. Applied Surface Science, 2017, 411, 144-148.	6.1	18
24	Hydrothermal synthesis, characterization and properties of TiO2 nanorods on boron-doped diamond film. Materials Letters, 2010, 64, 2012-2015.	2.6	17
25	Reduction of leakage current by O2 plasma treatment for device isolation of AlGaN/GaN heterojunction field-effect transistors. Applied Surface Science, 2015, 351, 1155-1160.	6.1	17
26	Quasi-vertical GaN heterojunction diodes with p-NiO anodes deposited by sputtering and post-annealing. Vacuum, 2020, 182, 109784.	3.5	17
27	Positive threshold voltage shift in AlGaN/GaN HEMTs with p-type NiO gate synthesized by magnetron reactive sputtering. Applied Surface Science, 2018, 462, 799-803.	6.1	16
28	Vertical GaN-Based Temperature Sensor by Using TiN Anode Schottky Barrier Diode. IEEE Sensors Journal, 2021, 21, 1273-1278.	4.7	16
29	Effect of nitrogen on deposition and field emission properties of boron-doped micro- and nano-crystalline diamond films. Nano-Micro Letters, 2010, 2, 154-159.	27.0	15
30	Synthesis of titanium nitride for self-aligned gate AlGaN/GaN heterostructure field-effect transistors. Nanoscale Research Letters, 2014, 9, 590.	5.7	15
31	Determination of band offsets between p-NiO gate electrode and unintentionally doped GaN for normally-off GaN power device. Journal of Alloys and Compounds, 2017, 728, 400-403.	5.5	15
32	Normally off AlGaN/GaN ion-sensitive field effect transistors realized by photoelectrochemical method for pH sensor application. Superlattices and Microstructures, 2019, 128, 99-104.	3.1	15
33	Evaluation of a Gate-First Process for AlGaN/GaN Heterostructure Field-Effect Transistors. Japanese Journal of Applied Physics, 2013, 52, 11NH01.	1.5	14
34	Effects of recess process and surface treatment on the threshold voltage of GaN MOSFETs fabricated on a AlGaN/GaN heterostructure. Semiconductor Science and Technology, 2015, 30, 065004.	2.0	12
35	The effect of CO2 on the high-rate homoepitaxial growth of CVD single crystal diamonds. Diamond and Related Materials, 2011, 20, 496-500.	3.9	11
36	Characterization of GaN MOSFETs on AlGaN/GaN Heterostructure With Variation in Channel Dimensions. IEEE Transactions on Electron Devices, 2014, 61, 498-504.	3.0	11

#	Article	IF	CITATIONS
37	The influence of Al composition in AlGaN back barrier layer on leakage current and dynamic R ON characteristics of AlGaN/GaN HEMTs. Physica Status Solidi (A) Applications and Materials Science, 2017, 214, 1600824.	1.8	11
38	Dependence of carbon doping concentration on the strain-state and properties of GaN grown on Si substrate. Superlattices and Microstructures, 2018, 120, 720-726.	3.1	10
39	GaN Schottky barrier diode with thermally stable nickel nitride electrode deposited by reactive sputtering. Materials Science in Semiconductor Processing, 2019, 93, 1-5.	4.0	10
40	GaN Schottky barrier diodes with nickel nitride anodes sputtered at different nitrogen partial pressure. Vacuum, 2019, 162, 72-77.	3.5	10
41	Transparent ohmic contact for boron doped diamond using p-type NiO film synthesized through oxidation. Materials Science in Semiconductor Processing, 2020, 105, 104740.	4.0	8
42	Correlating device behaviors with semiconductor lattice damage at MOS interface by comparing plasma-etching and regrown recessed-gate Al2O3/GaN MOS-FETs. Applied Surface Science, 2021, 546, 148710.	6.1	8
43	Analysis of electrical properties in Ni/GaN schottky contacts on nonpolar/semipolar GaN free-standing substrates. Journal of Alloys and Compounds, 2022, 898, 162817.	5.5	8
44	Effect of Anode Material on the Sensitivity of GaN Schottky Barrier Diode Temperature Sensor. IEEE Sensors Journal, 2022, 22, 1933-1938.	4.7	8
45	Normally-off AlGaN/GaN heterostructure junction field-effect transistors with blocking layers. Superlattices and Microstructures, 2018, 120, 448-453.	3.1	7
46	Vertical GaN Schottky barrier diodes with area-selectively deposited p-NiO guard ring termination structure. Superlattices and Microstructures, 2021, 151, 106820.	3.1	7
47	Design of bevel junction termination extension structure for high-performance vertical GaN Schottky barrier diode. Superlattices and Microstructures, 2021, 159, 107048.	3.1	7
48	Plasma-assisted ohmic contact for AlGaN/GaN heterostructure field-effect transistors. Semiconductor Science and Technology, 2016, 31, 035015.	2.0	6
49	Improvement of device isolation using field implantation for GaN MOSFETs. Semiconductor Science and Technology, 2016, 31, 035019.	2.0	6
50	A review of selective area grown recess structure for insulated-gate E-mode GaN transistors. Japanese Journal of Applied Physics, 2020, 59, SA0806.	1.5	6
51	Gate-first GaN MOSFET based on dry-etching-assisted non-annealing ohmic process. Applied Physics Express, 2015, 8, 046501.	2.4	5
52	Evaluation of a gate-first process for AlGaN/GaN metal-oxide-semiconductor heterostructure field-effect transistors with low ohmic annealing temperature. Chinese Physics B, 2016, 25, 038503.	1.4	5
53	Effect of overdrive voltage on PBTI trapping behavior in GaN MIS-HEMT with LPCVD SiN _x gate dielectric*. Chinese Physics B, 2020, 29, 037201.	1.4	5
54	Synthesis and Application of Metal Nitrides as Schottky Electrodes for Gallium Nitride Electron Devices. Science of Advanced Materials, 2014, 6, 1645-1649.	0.7	5

#	Article	IF	CITATIONS
55	Metal-oxide-semiconductor AlGaN/GaN heterostructure field-effect transistors using TiN/AlO stack gate layer deposited by reactive sputtering. Semiconductor Science and Technology, 2015, 30, 015019.	2.0	4
56	Influence of AlGaN back barrier layer thickness on the dynamic ron characteristics of AlGaN/GaN HEMTs. , 2016, , .		4
57	Plasma-assisted surface treatment for low-temperature annealed ohmic contact on AlGaN/GaN heterostructure field-effect transistors. Chinese Physics B, 2017, 26, 037201.	1.4	4
58	Impact of dislocation pits on device performances and interface quality degradation for E-mode recessed-gate Al2O3/GaN MOSFETs. Journal of Alloys and Compounds, 2021, 854, 157144.	5.5	4
59	Threshold Voltage Engineering in Al ₂ O ₃ /AlGaN/GaN MISHEMTs with Thin Barrier Layer: MIS-gate Charge Control and High Threshold Voltage Achievement. , 2021, , .		4
60	MoOx-Si heterojunction with wide-band-gap MoOx contact layer in the application of low-intensity visible-light sensing. Materials Science in Semiconductor Processing, 2021, 131, 105879.	4.0	4
61	Recessed-anode AlGaN/GaN diode with a high Baliga's FOM by combining a p-GaN cap layer and an an an an an an an	3.1	4
62	Surface sensibility and stability of AlGaN/GaN ion-sensitive field-effect transistors with high Al-content AlGaN barrier layer. Applied Surface Science, 2021, 570, 151190.	6.1	4
63	Field isolation for GaN MOSFETs on AlGaN/GaN heterostructure with boron ion implantation. Semiconductor Science and Technology, 2014, 29, 055002.	2.0	3
64	A balancing method for low Ron and high Vth normally-off GaN MISFET by preserving a damage-free thin AlGaN barrier layer. , 2018, , .		3
65	Influence of metal-insulator-semiconductor gate structure on normally-off p-GaN heterojunction field-effect transistors. Journal of Crystal Growth, 2020, 532, 125395.	1.5	3
66	Physical-Based Simulation of the GaN-Based Grooved-Anode Planar Gunn Diode. Micromachines, 2020, 11, 97.	2.9	3
67	Effect of geometry on the sensing mechanism of GaN Schottky barrier diode temperature sensor. IEICE Electronics Express, 2021, 18, .	0.8	3
68	Vertical GaN Shottky barrier diode with thermally stable TiN anode*. Chinese Physics B, 2021, 30, 038101.	1.4	3
69	Ohmic and Schottky contacts of hydrogenated and oxygenated boron-doped single-crystal diamond with hill-like polycrystalline grains*. Chinese Physics B, 2021, 30, 096803.	1.4	3
70	Evaluation of stress voltage on off-state time-dependent breakdown for GaN MIS-HEMT with SiN x gate dielectric. Chinese Physics B, 2020, 29, 107201.	1.4	3
71	Charge Control in Schottky-Type p-GaN Gate HEMTs With Partially and Fully Depleted p-GaN Conditions. IEEE Transactions on Electron Devices, 2022, 69, 2262-2269.	3.0	3
72	Growth and Characteristics of Freestanding Hemispherical Diamond Films by Microwave Plasma Chemical Vapor Deposition. Chinese Physics Letters, 2010, 27, 047802.	3.3	2

#	Article	IF	CITATIONS
73	A self-aligned gate GaN MOSFET using an ICP-assisted low-temperature Ohmic process. Semiconductor Science and Technology, 2015, 30, 075003.	2.0	2
74	GaN metal-oxide-semiconductor field-effect transistors on AlGaN/GaN heterostructure with recessed gate. Frontiers of Materials Science, 2015, 9, 151-155.	2.2	2
75	A novel normally-off GaN MISFET with an in-situ AlN space layer using selective area growth. , 2016, , .		2
76	Self-aligned-gate AlGaN/GaN heterostructure field-effect transistor with titanium nitride gate. Chinese Physics B, 2016, 25, 087308.	1.4	2
77	Synthesis of thermally stable HfO x N y as gate dielectric for AlGaN/GaN heterostructure field-effect transistors. Chinese Physics B, 2018, 27, 078503.	1.4	2
78	Thermal Analysis of AlGaN/GaN Hetero-Structural Gunn Diodes on Different Substrates Through Numerical Simulation. IEEE Journal of the Electron Devices Society, 2020, 8, 134-139.	2.1	2
79	Experimental evaluation of interface states during time-dependent dielectric breakdown of GaN-based MIS-HEMTs with LPCVD-SiN x gate dielectric. Chinese Physics B, 2020, 29, 067203.	1.4	2
80	Recent Progress on Photoelectrochemical Water Splitting of Graphitic Carbon Nitride (gâ^'CN) Electrodes. Nanomaterials, 2022, 12, 2374.	4.1	2
81	The breakdown behavior of GaN epitaxial material on silicon. , 2016, , .		1
82	Influence of interface contamination on transport properties of two-dimensional electron gas in selective area growth AlGaN/GaN heterostructure. Journal of Materials Science: Materials in Electronics, 2016, 27, 9061-9066.	2.2	1
83	Enhanced voltage blocking ability of AlGaN/GaN heterojunction FETs-on-Si by eliminating leakage path introduced by low-temperature-AlN interlayers. Japanese Journal of Applied Physics, 2017, 56, 065503.	1.5	1
84	Understanding of impact of carbon doping on background carrier conduction in GaN*. Chinese Physics B, 2021, 30, 107201.	1.4	1
85	Band alignment between NiO x and nonpolar/semipolar GaN planes for selective-area-doped termination structure*. Chinese Physics B, 2021, 30, 067701.	1.4	1
86	Hybrid-anode structure designed for a high-performance quasi-vertical GaN Schottky barrier diode. Chinese Physics B, 2022, 31, 057702.	1.4	1
87	Influence of the Groove Depth on the Electrical Characteristics of the Vertical GaN Trench MOSFETs. , 2020, , .		1
88	Effect of Gan interlayer thickness on the Algan/Gan heterostructure field-effect transistors for self-terminated wet etching process. , 2016, , .		0
89	Influence of the Aln/Gan superlattices buffer thickness on the electrical properties of Algan/Gan HFET on Si substrate. , 2016, , .		0
90	GaN Schottky Barrier Diodes with TiN Electrode for Microwave Power Transmission. Materials Science Forum, 2019, 954, 126-132.	0.3	0

#	Article	IF	CITATIONS
91	Breakdown Mechanism of AlGaN/GaN-based HFET With Carbon-doped GaN Buffer Layer grown on Si substrate. , 2019, , .		0
92	Study on Self-Parallel GaN-Based Terahertz Hetero-Structural Gunn Diode. Applied Sciences (Switzerland), 2020, 10, 5777.	2.5	0
93	Normally-Off GaN Power Device Based on Stack AlGaN Barrier Structure and P-Type NiO Gate Electrode. Materials Science Forum, 0, 1014, 86-92.	0.3	0
94	Metal-nitride dual-anode AlGaN/GaN heterostructure Schottky barrier diodes with tunable turn-on voltage and reverse leakage current. Semiconductor Science and Technology, 2022, 37, 045013.	2.0	0
95	Determination of band alignment between GaOx and boron doped diamond for selective-area-doped termination structure. Chinese Physics B, 0, , .	1.4	0